UC Davis

UC Davis Previously Published Works

Title

Effect of van der Waals interactions on the chemisorption and physisorption of phenol and phenoxy on metal surfaces.

Permalink

https://escholarship.org/uc/item/2kh206rw

Journal

The Journal of chemical physics, 145(10)

ISSN

0021-9606

Authors

Peköz, Rengin

Donadio, Davide

Publication Date

2016-09-01

DOI

10.1063/1.4962236

Peer reviewed

eScholarship.org Powered by the California Digital Library
University of California

Effect of van der Waals Interactions on the Chemisorption and Physisorption of Phenol and Phenoxy on Metal Surfaces

Rengin Peköz[1, a)] and Davide Donadio[2]
[1)] *Department of Electrical and Electronics Engineering, Atılım University, 06836 Ankara, Turkey*[b)]
[2)] *Department of Chemistry, University of California Davis, One Shields Avenue, Davis, CA, 95616, U.S.A*[b)]

(Dated: 28 July 2016)

The adsorption of phenol and phenoxy on the (111) surface of Au and Pt has been investigated by density functional theory calculations with the conventional PBE functional and three different non-local van der Waals (vdW) exchange and correlation functionals. It is found that both phenol and phenoxy on Au(111) are physisorbed. In contrast phenol on Pt(111) presents an adsorption energy profile with a stable chemisorption state and a weakly metastable physisorbed precursor. While the use of vdW functionals is essential to determine the correct binding energy of both chemisorption and physisorption states, the relative stability and existence of an energy barrier between them depends on the semi-local approximations in the functionals. The first dissociation mechanism of phenol, yielding phenoxy and atomic hydrogen, has been also investigated, and the reaction and activation energies of the resulting phenoxy on the flat surfaces of Au and Pt were discussed.

Keywords: (Meta)stable states; Metal–organic interfaces; Density functional theory; Dispersion forces

I. INTRODUCTION

The interactions between aromatic molecules and transition-metal surfaces play an essential role in controlling the selectivity and activity of metal-catalyzed reactions. Among aromatic molecules, phenol (C_6H_5OH) and phenoxy (C_6H_5O, O-H bond dissociation product of phenol) are key players in polymer-metal interface chemistry, not only because they are subunits of polyimides, but also because they often occur as byproducts in industrial processes. Phenolic groups have been used as adhesion promoters which serve to enhance the adhesive bonding between organic films and metal surfaces.[1] Phenol is also important in chemical industry in the production of various materials such as bisphenol, phenolic sulfonic acid and adipic acid.[2] Furthermore, since phenol has multiple bonds leading to molecular adsorption and O-H bond, which breaks and forms a metal-O bond, it is interesting to figure out which adsorption processes is prevailing. The type of the bonding behavior will lead to different adsorption structures and consequently reactivity.

Although the adsorption of phenol (PL) and phenoxy (PX) on metal surfaces have been extensively studied experimentally , e.g. on Cu(110),[3,4] Mo(110),[5,6] Rh(111),[7] Ag(110)[8] and Ag(111),[9] Ni(110),[10,11] Ni(111),[12] Pd(110),[13] Au(111),[14] and Pt(111),[15,16] theoretical studies are limited to Rh(111) and Pt(111),[17,18] Ni(111), Ni(110) and Ni(221),[19,20] and Pd(111).[18,21] Most of these studies reported that while the C-ring of PL and PX was nearly parallel to the surface plane on Cu(110),[3] Ni(111),[12] and Pt(111),[16] PX has tilted geometries on Ag(110)[8] and Mo(110).[6] Scanning tunneling microscopy (STM) showed that the local coverage of PX on Cu(110) results in different ring orientations: nearly parallel for 0.25 and almost normal to the surface plane for 0.33 PX per surface Cu atom.[4]

In an early study the adsorption of phenol on polycrystalline Au was investigated by capacitance and modulated reflectance measurements.[22] While this study showed that PL was predominantly adsorbed with a flat configuration, they also revealed the occurrence of flat to vertical reorientation, in which PL is attached to the metal via its oxygen atom. Another investigation on Au(111) by STM and infrared spectroscopy suggested that PL keeps its C-ring parallel to the surface with 30° angle with respect to the underlying Au(111) lattice with no specific adsorption site, and PX binds to the surface through the O atom.[14] These observations suggest the possibility that molecules are observed in metastable or precursor states, which are preliminary to chemisorption. While several theoretical models were developed to predict experimental molecular sticking coefficients,[23,24] a precursor state was first directly observed by Brown and his coworkers for benzene adsorbed on Si(111).[25] Recently, theoretical calculations have also predicted the bistability of graphene on Ni(111)[26] and benzene derivatives on Pt(111).[27–29]

In this Article, the interaction of phenol and phenoxy with Au(111) and Pt(111) surfaces is investigated using density functional theory (DFT) calculations. To explore the effect of the substrate, Au and Pt substrates are chosen because of their different electronic structures, i.e, fully occupied d-band and partially occupied d-band, respectively. Since the interaction between organic molecules and metal surfaces involves a significant contribution of dispersion forces, we consider different

[a)] Electronic mail: rengin.pekoz@atilim.edu.tr
[b)] Max Planck Institute for Polymer Research, Ackermannweg 10, 55128 Mainz, Germany

flavors of non-local van der Waals functionals (vdW-DF and vdW-DF2),[30–32] and we compare the results to those obtained using standard generalized gradient approximation (GGA) functionals, such as PBE.[33,34]

Our calculations suggest that phenol and phenoxy on Pt(111) exhibit a chemisorption state and a weakly metastable precursor physisorption state. In contrast, there is only one adsorption minimum for both molecules on Au(111). Benchmark calculations of benzene on Au and Pt(111) surfaces yield that the experimental adsorption energies and distances are captured by vdW-DF2 and vdW-DF combined with PBE exchange. The inclusion of vdW flavors is essential to get the physisorption energies of molecules on Au and Pt(111) surfaces. In turn we find that chemisorption energies strongly depend on the type of vdW functional used. Moreover, using the original vdW-DF and vdW-DF2 functionals yields higher energy barriers compared to the PBE and modified vdW-DF functionals. These results show that the relative strength of these chemisorbed and physisorbed states and the energy barrier strongly depend on the type of metal and functional used. Furthermore, the first step in the decomposition of phenol into phenoxy, i.e.,the O-H bond dissociation which is similar to adsorbed alcohols, on Au(111) and Pt(111) surfaces is also calculated, and the mechanism and energetics will be discussed.

II. COMPUTATIONAL METHODS

The adsorption energy and geometry of phenol (PL) and phenoxy (PX) molecules on Au(111) and Pt(111) are computed by density functional theory (DFT). Van der Waals (vdW) forces provide a significant contribution to the interaction of aromatic molecules with transition metal surfaces. Since the local nature of the correlation part of standard GGA functionals does not entail dispersion forces, we need to consider functionals that account properly for vdW interactions.[30,35–38] Actually, a thorough comparison between results obtained using local GGA functionals, such as PBE,[33,34] and various flavors of van der Waals density functionals[30–32] allows us to capture the importance of vdW interactions, and to assess the accuracy of the latter functional. We employed the following vdW functionals: the van der Waals density functional (vdW-DF) with revPBE exchange,[30] (denoted as revPBE-vdW), vdW-DF with PBE exchange (denoted as PBE-vdW),[31] and the vdW-DF2[32] with the original PW86 exchange (denoted as PW86-vdW2).[39] vdW-DF2 is similar to vdW-DF, but both the exchange and nonlocal correlation parts have been changed to improve the binding description using a more accurate kernel. Core electrons were replaced by projector augmented wave (PAW) pseudopotentials.[40,41] A cutoff energy of 400 eV for the plane-wave basis set was employed. First-principles calculations were performed using the Vienna *ab initio* simulation package (VASP) version 4.2.[42,43]

The optimized equilibrium lattice constants of bulk Pt(Au) are 3.98(4.17), 4.03(4.23), 4.05(4.27) and 4.13(4.35) Å using PBE, PBE-vdW, revPBE-vdW and PW86-vdW2, respectively. These calculated lattice constants are in good agreement with the previously reported values.[44,45] In general, vdW-DF functionals give larger lattice constants than conventional PBE and experimental value of 4.07 and 3.92 Å for Au and Pt, respectively, which is in agreement with the finding of other transition metals.[44] The largest error obtained, compared to the experimental values, is for PW86-vdW2 functional which is a very repulsive functional for small separations.[46]

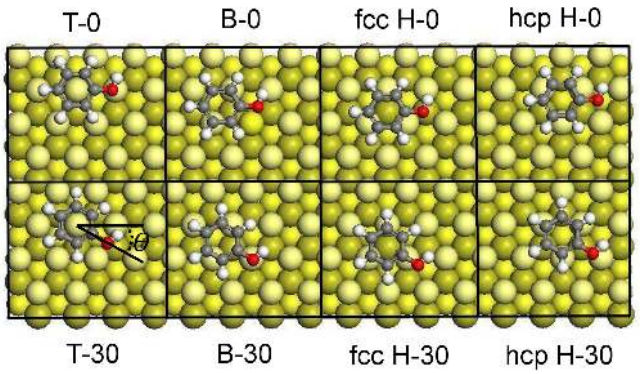

FIG. 1. *Initial* high-symmetry adsorption geometries of phenol on Au(111). The center of the C-rings are located on the top (T), bridge (B), fcc and hcp hollow (H) sites. The O-H position with respect to the surface is given by the azimuthal angle between molecule and the direction of Au rows. The black lines indicate the unit cell of Au(111).

The adsorption energies of molecules adsorbed at the surface of metal slabs were tested against the thickness of the slab. PL and PX adsorption energies on Au(111) are well converged for four atomic layers thick slabs, and change only by 0.03 eV increasing the thickness to six atomic layers. In turn, the chemisorption energies of PL and PX on Pt(111) converge only for slabs as thick as six atomic layers. For this reason we use six atomic layers of Pt in all the calculations, unless otherwise noted. The surfaces were modeled with a c(2x4) supercell, having 16 surface atoms per slab. The two surface metal layers were allowed to relax, while the rest of layers were fixed at the calculated bulk positions. The replicated images of the cells were separated by about 20 Å in the direction perpendicular to the surfaces. The first Brillouin zone was sampled on a 4x4x1 regular grid of k-points.[47] The Fermi level was smeared using the Methfessel and Paxton method[48] with a width of 0.2 eV. All structures were optimized with a convergence criterion of 10 meV/Å for the forces and 0.1 meV for the energy. The convergence of the present settings, including the thickness of the vacuum and k-point sampling, was analyzed. Increasing the vacuum region from 20 to 40 Å decreased the adsorption energy by 0.009 eV, and using a denser k-point mesh (6x6x1) changed the adsorption energy by 0.003

and 0.005 eV for four and six atomic layers thick slabs of Au and Pt(111) surfaces, respectively.

The adsorption energy of the molecule, $E_{\rm ads}$, is defined as:

$$E_{\rm ads} = E_{tot} - (E_{surf} + E_{mol}), \quad (1)$$

where E_{tot}, E_{surf} and E_{mol} are the total energies of the relaxed adsorbed system, the clean metal surface, and the isolated molecule, respectively. A negative value of $E_{\rm ads}$ means that the adsorbed system is energetically favorable relative to the isolated state. The eight high symmetry adsorption sites for PL and PX on flat surface are displayed in Fig. 1. The adsorption energy profiles (AEP) of benzene (BZ), PL and PX on metal surfaces are calculated for the most stable adsorption sites.[?] Since BZ and PL keep their C-ring planar, AEP curves for BZ and PL on Au and Pt(111) surfaces are calculated by fixing the coordinates of the two opposite carbon atoms, one is attached to the oxygen atom for the PL case, and adjusting the average C-ring vertical distance (z) from the surface. On the other hand, PX on Au(111) prefers to bind to the surface via its O atom, thus AEP is calculated by adjusting the O-Au vertical distance and fixing the z-coordinate of O atom. For the adsorption of PX on Pt(111) surface n^5-π-like binding takes place, thus we followed the same way described for PL on surfaces.[49] Since AEPs are computed applying constraints, they are an upper limit to the energetics.

The energy barrier for the transition from PL into PX and atomic hydrogen on Au(111) and Pt(111) surfaces was calculated using the nudge elastic band (NEB) method[50,51] implemented in the VASP code. The most favorable adsorption sites for PL and PX on the metal surfaces were considered, and the adsorption site for atomic hydrogen was chosen as fcc-hollow site which is the most stable adsorption site proposed by previous studies.[52–54]

III. RESULTS AND DISCUSSION

We discuss the adsorption of phenol, the reaction pathway for the dissociation of phenol into phenoxy, and the adsorption of phenoxy on Au(111) and Pt(111) using conventional PBE functional and those obtained with vdW-DF exchange and correlation functionals. Our goal is to understand the effect of vdW interactions on the adsorption features and to explore the performance of the chosen vdW functionals. Furthermore, we aim at investigating the effect of the substrate used in the adsorption properties, and to elucidate the reasons for the bistable adsorption found of phenol on Pt(111), in contrast to adsorption on Au(111). In the first subsection, we briefly discuss the adsorption of benzene (BZ) on Au(111) and Pt(111) as a benchmark system to validate the set-up and the functionals used. We then discuss the adsorption energies and geometries of phenol, such as the adsorption heights and the structural changes in the molecule upon adsorption, and compare the results within different functionals used and to the available data in the literature. In section 3.3, we summarize the adsorption properties of phenoxy on Au(111) and Pt(111) using different functionals and if available compare with the literature. We then explore the dissociation of phenol into phenoxy and discuss the reaction pathways on Au(111) and Pt(111). In section 3.5, we will discuss the modifications on the electronic structure upon adsorption.

The results presented here, concerning the adsorption and chemical reactions at Au and Pt(111) surfaces, are convincing in the sense that the applied methods have been shown to yield a good description of such properties of several similar systems.[45? ?]

A. Benchmark Calculations on Benzene

The adsorption of benzene on Au(111) and Pt(111) surfaces was previously studied using PBE, vdW-DF with PBE and revPBE, and vdW-DF2 with PW86 exchange.[28] It was found that the most favorable adsorption sites for benzene on Au(111) and Pt(111) are hcp-hollow and bridge, respectively, where the C-ring parallel to the surface was 30° with respect to the underlying lattice, in agreement with other studies.[27,55] The comparison of the calculated adsorption energies to the experimental and other calculated data are presented in Table S1 of the supplementary material.[56] To shed light on the differences in the adsorption mechanism of benzene on Au(111) and Pt(111) surfaces, we have calculated the adsorption energy profile (AEP), obtained with PBE and three different vdW functionals and shown in Figure S1 of the supplementary material.[56] The comparison shows that different functionals yield good agreement with the experimental data for Au(111) and Pt(111) surfaces. While PW86-vdW2 gives the best agreement with the experiments on Au(111), the adsorption features of BZ on Pt(111) are better reproduced by the PBE-vdW functional. Moreover, AEP also demonstrates the effect of dispersion forces at short and long binding distances. The chemisorption and physisorption states of BZ on Pt(111) are captured by all the functionals used here. PBE gives negligible physisorption energy ($E_{\rm ads}^{\rm phys}$) for BZ on Au(111) and Pt(111) surfaces, while the inclusion of vdW interactions, regardless of which functional is used, significantly enhances the $E_{\rm ads}^{\rm phys}$. The strength of $E_{\rm ads}^{\rm phys}$ is in the order PBE < revPBE-vdW < PW86-vdW2 < PBE-vdW on both surfaces. On the other hand, with the addition of different vdW flavors the chemisorption energy of BZ on Pt(111) surface exhibits large variations. PBE yields a stronger chemisorption energy compared to revPBE-vdW and PW86-vdW2 functionals, as seen in previous studies.[45,57] This result is due to the repulsive nature of revPBE-vdW and PW86-vdW2 at short distances.

Furthermore, not only the energy barrier between the physisorbed and chemisorbed states, but also the relative

stability of these states on Pt(111) are different for different vdW flavors (see Figure S1 of the supplementary material[56]). Both PBE and PBE-vdW predict that the barrier from physisorption to chemisorption state essentially vanishes, whereas the potential energy barrier calculated using revPBE-vdW and PW86-vdW2 functionals is more significant.[45]

A comparison with experimental measurements[58] and calculations using other approaches[45] suggests that among the functionals considered PBE-vdW is the best compromise, as it reproduces reasonably well energy of BZ both physisorbed at Au(111) and chemisorbed at Pt(111). In turn PW86-vdW2 is the most accurate for physisorption energies, but largely underestimates chemisorption.

B. Adsorption Energy and Equilibrium Geometry of Phenol on Au(111) and Pt(111)

We consider PL on Au(111) and Pt(111) at eight high symmetry adsorption sites (see Fig. 1) using PBE and PBE-vdW for flat-lying orientations. Non-parallel orientations of phenol on surfaces, which become important for coverages greater than 2 monolayers (ML),[16] are not considered in this work. The preliminary calculations for finding the most favorable adsorption sites are performed by using a four atomic layer of Au and Pt metals.

1. PL/Au(111)

Both PBE and PBE-vdW predict that PL prefers to sit on hcp-30 site on Au(111), as found for BZ on Au(111). Similar to BZ adsorbed on Au(111), PL has only physisorption state on Au(111). Almost identical adsorption energies are found for different adsorption sites (see Table S2 and Figure S2 of the supplementary material[56]), with the maximum $E_{\rm ads}^{\rm phys}$ difference being 0.05 and 0.12 eV for PBE and PBE-vdW, respectively, indicating that the diffusion barrier of PL on Au(111) surface might be small. Using the most favorable adsorption sites found with PBE and PBE-vdW (hcp-30),[59] the adsorption properties of PL on Au(111) are further calculated using revPBE-vdW and PW86-vdW2 functionals. The inclusion of vdW interactions with any type of functional enhances the adsorption energy compared to PBE (see Fig. 2(a) and Table I). Whereas the smallest enhancement in the $E_{\rm ads}^{\rm phys}$ is found using revPBE-vdW (by 0.52 eV), the largest is obtained using the PBE-vdW functional (by 0.85 eV). As summarized in Table I, the calculated adsorption energies for PL/Au(111) system have the sequence of PBE < revPBE-vdW < PW86-vdW2 < PBE-vdW, ranging from -0.12 to -0.97 eV. This adsorption energy order is the same as the one found for BZ adsorbed on Au(111) surface.

On the hcp-30 site, PL is adsorbed parallel to Au(111) surface with the center of C-ring on hcp site and O atom is atop site. The deformation energy of a molecule ($E_{\rm def}$) is calculated as the single point energy difference of a molecule in its adsorbed configuration and a relaxed molecule in vacuum in the same simulation box. $E_{\rm def}$ for PL on Au(111) is around 4 meV for all functionals, which confirms that PL on Au surface retains its gas-phase configuration. We define the adsorption height as the average distance between the C-ring of PL and the top layer of the metal surface (d_{C-S}). While PBE predicts the largest d_{C-S} being 3.40 Å, the inclusion of vdW interactions decreases the adsorption height by 0.09-0.26 Å. Among the vdW implementations, PW86-vdW2 functional brings PL molecule the closest to Au(111) surface with d_{C-S} equal to 3.14 Å, while revPBE-vdW gives the largest adsorption height (d_{C-S} = 3.31 Å). Deformation energies and further geometrical details are presented in Table S3 of the supplementary material.[56]

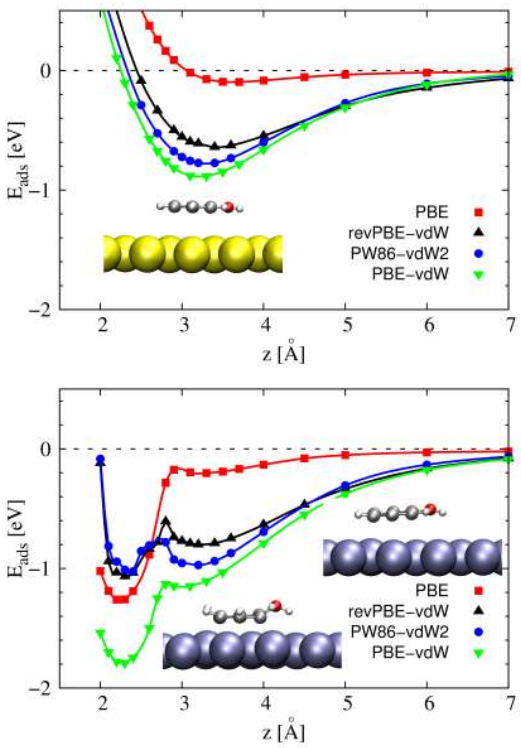

FIG. 2. Calculated adsorption energy of a phenol molecule on Au(111) and Pt(111) surfaces with different exchange-correlation functionals as a function of distance between the surface and the center of the molecule. The insets show the chemi- and physisorbed configurations.

2. PL/Pt(111)

While PL is physisorbed on Au(111), its adsorption on Pt(111) exhibits both chemisorbed and physisorbed states (see Fig. 2), similar to the adsorption of benzene on these two surfaces. PBE predicts the most favorable physisorption site as B-30, while PBE-vdW gives hcp-

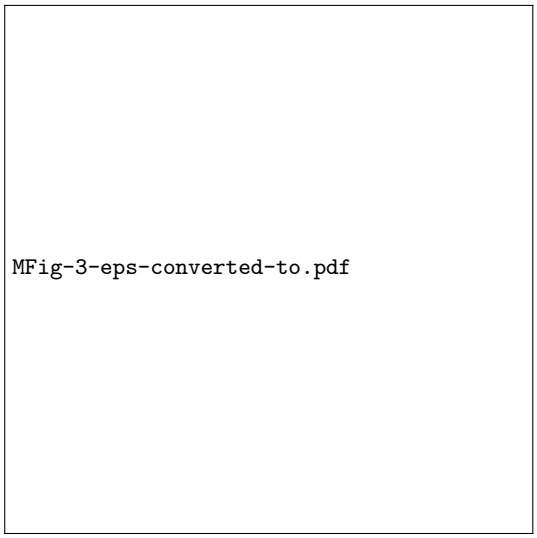

FIG. 3. Calculated adsorption energy of a phenoxy molecule on Au(111) and Pt(111) surfaces with different exchange-correlation functionals as a function of distance between the surface and the center of the molecule. The insets show the chemi- and physisorbed configurations.

30 site. These two adsorption sites have been further checked for the other vdW functionals,[60] and in the following discussions, hcp-30 site is accepted to be the most favorable physisorption site for all vdW functionals, while B-30 is energetically the most stable one for PBE calculation. The relaxed physisorbed configurations of PL on Pt(111) are presented in Figure S3 of the supplementary material.[56]

Comparing PBE to PBE-vdW for the physisorbed states shows that the inclusion of vdW increases the $E_{\rm ads}^{\rm phys}$ by 0.87 eV. The other vdW functionals, revPBE-vdW and PW86-vdW2, give lower $E_{\rm ads}^{\rm phys}$ than that of PBE-vdW, but stronger than PBE by 0.43 and 0.63 eV, respectively. The analysis of the equilibrium geometries of physisorbed PL on Pt(111) shows that the average distance between Pt surface atoms and C-ring obtained from PBE-vdW is the smallest (2.80 Å) and revPBE-vdW, which is repulsive in nature, gives the largest adsorption height (3.19 Å). The geometrical details are collected in Table S3 of the supplementary material.[56] In its physisorbed state on Pt(111), PL keeps its gas phase geometry for all vdW included calculations. The energy difference between the different adsorption sites for physisorbed state indicates that the predicted energy barrier for the diffusion of physisorbed PL on Pt(111), using both PBE and PBE-vdW, might be around 0.21 eV.

The effect of using different functionals on the adsorption energies of physi- and chemisorption states of PL on Pt(111) surface and their relative strength can be deduced from Fig. 2 and Table I. Conventional PBE and PBE-vdW give a small energy barrier from physisorption to chemisorption states (0.03 eV), and the chemisorption energies are much deeper than the physisorption energies

TABLE I. Comparison of the calculated chemisorption ($E_{\rm ads}^{\rm chem}$) and physisorption energies ($E_{\rm ads}^{\rm phys}$) of phenol and phenoxy on Au(111) and Pt(111). The most favorable adsorption sites, reported in Table S2 and Table S4 of the supplementary material,[56] are used for PBE and PBE-vdW calculations, and for the other vdw functionals the adsorption sites found by PBE-vdW functional are used. Energies are in eV.

System	Method	$E_{\rm ads}^{\rm phys}$	System	$E_{\rm ads}^{\rm chem}$	$E_{\rm ads}^{\rm phys}$
BZ/Au	PBE	-0.08	BZ/Pt	-1.35	-0.16
	PBE-vdW	-0.81		-1.76	-1.05
	revPBE-vdW	-0.55		-1.06	-0.67
	PW86-vdW2	-0.65		-0.99	-0.81
PL/Au	PBE	-0.12	PL/Pt	-1.31	-0.36
	PBE-vdW	-0.97		-1.82	-1.23
	revPBE-vdW	-0.64		-1.09	-0.79
	PW86-vdW2	-0.77		-1.04	-0.99
PX/Au	PBE	-0.73	PX/Pt	-2.39	-1.12
	PBE-vdW	-1.51		-2.87	-1.93
	revPBE-vdW	-1.09		-2.20	-1.49
	PW86-vdW2	-1.29		-2.11	-1.65

by 0.95 and 0.59 eV, respectively. On the other hand, using revPBE-vdW and PW86-vdW2 functionals significantly decreases the energy difference between physi- and chemisorption states by 0.3 and 0.05 eV, and increases the energy barrier by 0.19 and 0.31 eV, respectively.

The chemisorbed configuration of PL on Pt(111) shows that PL is distorted from its gas phase geometry with the C-ring closely parallel to the surface, the C-H and C-O bonds bend upward, and the H atom in the OH bond bends downward, which is shown in Fig. 2(b). Both PBE and PBE-vdW find that the B-30 site is the most stable one, consistent with the findings of experimental[16] and theoretical studies.[17,18] Thus B-30 site is considered for the other vdW calculations presented in this work. The calculated $E_{\rm def}$ confirms the large distortions obtained in the chemisorption states compared to the gas-phase counterpart of PL which are tabulated in Table S3 of the supplementary material.[56] The largest deformation energy is calculated for PBE (1.81 eV) and the smallest one for PBE-vdW (1.69 eV). The average distance between the C-ring and Pt surface is between 2.15 and 2.20 Å, consistent with former studies.[17,18] The energetics and geometrical details are given in Table S2 and Figure S4 of the supplementary material.[56]

The effect of vdW flavors on chemisorption energies is different than those of the previously discussed cases for the physisorption of PL on Au and Pt surfaces. The conventional PBE functional predicted the adsorption energy of B-30 site using six (four) Pt slabs to be -1.31 (-1.14) eV which is in agreement with another DFT study.[18] Compared to PBE, the inclusion of vdW forces using the PBE exchange favors the $E_{\rm ads}^{\rm chem}$ by 0.51 eV, while using the same vdW-DF with revPBE and vdW-DF2 with PW86 exchange destabilizes chemisorption energy by 0.22 and 0.27 eV, respectively. The reason, as previously mentioned for BZ/Au(111), is the repulsive nature of revPBE-vdW and PW86-vdW functionals at

short range.

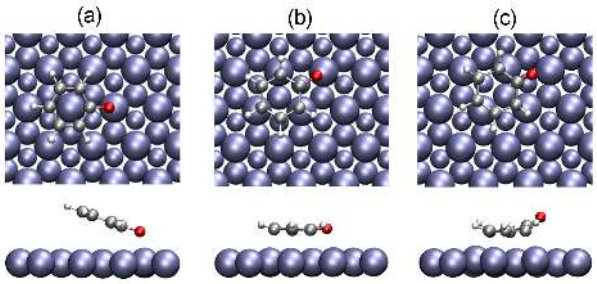

FIG. 4. Possible PX adsorption geometries on Au(111) and Pt(111) surfaces. (a) σ-like, (b) n^6-π-like, and (c) n^5-π-like adsorptions.

C. Adsorption Energy and Equilibrium Geometry of Phenoxy on Au(111) and Pt(111)

Three different adsorption configurations of PX on metal surfaces may occur: σ-adsorption via oxygen, n^5-π- and n^6-π-adsorption, shown in Fig. 4. In the σ-adsorption via oxygen configuration PX is tilted out of the surface, while n^5-π and n^6-π geometries entail π-bonding between the C-ring and surfaces, with five and six C atoms involved in the interaction, respectively. In the n^6-π configuration PX lies parallel to the surface, while for n^5-π the unbounded C with O atom bend up.

Likewise PL, the adsorption of PX on Au(111) and Pt(111) surfaces is studied for eight high symmetry adsorption sites using PBE and PBE-vdW functionals for flat-lying orientations. Vertical orientations of phenoxy on surfaces are not investigated.[17,18]

1. PX/Au(111)

Most of the investigated adsorption sites of PX on Au(111) using PBE and PBE-vdW functionals are found to be not stable. The molecule moves and/or tilts so that the oxygen atom binds to the surface gold atom, forming a σ-like adsorption as shown in the inset of Fig. 3(a). Both functionals find that PX prefers to sit on hcp-30 site on Au(111) and the molecule is tilted with an angle of $\sim$20° away from the surface. Using this most favorable adsorption site, the AEP of PX has been investigated in detail with PBE and vdW functionals (see Fig. 3(a)). For the AEP calculations of PX, the vertical distance between O atom and Au surface has been kept fixed and the rest of the system has been relaxed. It is found that there is only one adsorption minima for all functionals which is around $d_{(O-Au)} = 2.25$ Å, which reveals that an O-Au bond is formed. Compared to the adsorbed PL on Au(111), the distance between O atom and the closest surface Au atom decreases significantly by 0.98-1.25 Å. As a result, the interaction of PX with Au(111) gets stronger by $\sim$0.5 eV compared to that of PL. Fully relaxing the structures shows that PBE gives the smallest adsorption energy of -0.73 eV and revPBE-vdW and PW86-vdW2 follow with -1.09 and -1.29 eV, and the largest adsorption energy found by PBE-vdW being -1.51 eV. These figures indicate that even if the oxygen atom forms a chemical bond with the surfaces, vdW interactions provide a substantial contribution to the binding energy of PX on Au(111) and cannot be neglected. The bonding order is the same as for BZ and PL on Au(111). More details on the energetics, structural parameters and configurations are reported in Table S4 and S5 and Figure S2 of the supplementary material.[56]

2. PX/Pt(111)

The systematic investigation of the most stable chemisorption configuration shows that most of the sites have converted to either B-30 or hollow-30 sites after relaxation (see Table S4 of the supplementary material[56]). In the most favorable chemisorption state calculated by PBE and PBE-vdW, which is B-30 site, PX on Pt(111) keeps its C-ring almost parallel to the surface via five C atoms and the remaining C atom bonded to O atom is lifted up due to the strong repulsion between O-atom and Pt surface. This configuration is n^5-π-like and the relaxed structure is presented in the inset of Fig. 3(b). The calculated $E_{\rm ads}^{\rm chem}$ with PBE and PBE-vdW are equal to -2.23 (-2.39) and -2.72 (-2.87) eV for four (six) slabs, respectively. The geometrical details of PX on Pt(111) are very similar for both of the functionals, which are presented Table S4 and Figure S4 of the supplementary material.[56] Therefore, we only considered B-30 site for the other calculations including vdW functionals. The average distance between C-ring and surface Pt atoms is $\sim$2.23 Å, which is only 0.06 Å larger than the chemisorption state of PL on Pt(111). On the other hand, the distance between the O atom of PX and the closest surface Pt atom is 3.53 Å for PBE and 3.38 Å for PBE-vdW, which is 0.42 and 0.23 Å larger than the O-Pt distance of PL, respectively. The bonding order is PW86-vdW2 $<$ revPBE-vdW $<$ PBE $<$ PBE-vdW, with chemisorption energies of other vdW flavors -2.11 and -2.20 eV, respectively.

The AEPs calculated for B-30 site with PBE and PBE-vdW functionals show that there is no physisorption state of PX on Pt(111) with B-30 adsorption site. To have a more detailed analysis, the initial distance between PX and Pt(111) have been set to physisorption configuration for the other adsorption sites and fully relaxed configurations have been investigated. It is found that the relaxed configurations have either gone to chemisorption state or converted to different sites. However, T-0 site is an exception to this conversion and kept its physisorbed state with a σ-like adsorption via its O-atom to the surface Pt atom. More details on the energetics and structural information can be found in Table S4 and S5 and Figure

S5 of the supplementary material.[56]

D. Reaction Pathways

PL adsorbs with the C-ring parallel to the Au(111) and Pt(111) surfaces, and upon heating the O-H bond breaks first at 255 K for Pt(111) surface.[16] In order to understand the reaction pathways of the dissociation of phenol to coadsorbed phenoxy and H atom on Au(111) and Pt(111), we start with the most favorable adsorption sites of PL and PX as initial and the main final products of the reaction paths, respectively, on these surfaces. The dissociation reaction of PL into PX is studied for the chemisorption (physisorption) state of PL on Pt (Au) surface. Reaction pathway calculations have been carried out with PBE and PBE-vdW functionals, and four layer slabs have been used due to the computational cost. As previously mentioned, PX bonds to the Au surface via its O atom with a tilted geometry away from the surface. On the other hand, PX on Pt(111) has a n^5-π adsorption geometry. Both the transition state and the product have deprotonated states where the dissociated atoms are treated as atomic hydrogen. The dissociated hydrogen atom is adsorbed on fcc site for both surfaces, as suggested by previous studies.[28,61] For the sake of simplicity, the most favorable adsorption site of PL is called the initial state (IS) and the most favorable adsorption site of PX coadsorbed with a hydrogen atom is called the final state (FS). The initial guesses of the reaction pathways, with four reaction intermediates, were generated with the linear interpolation of IS and FS structures.[62]

The reaction energy (E_{reac}) is defined as the total energy difference between the IS and FS. The reaction energy of the dissociation of PL into coadsorbed PX and H atom on Au(111) and Pt(111) calculated by PBE-vdW is about 1.36 and 0.23 eV, respectively, which indicate that the reaction is endothermic on both surfaces (see Figure S6 of the supplementary material[56]). The present E_{reac} for Pt(111) is very similar to the previously reported data (0.26 eV).[17,18] These results reveal that the dissociation of phenol into coadsorbed phenoxy and H atom is thermodynamically unfavorable on both Au(111) and Pt(111).

The activation energy (E_a) is calculated as the total energy difference between the IS and the transition-state (TS) structure. The energy required to break O-H bond is E_a=1.50 and 0.34 eV on Au(111) and Pt(111), respectively. Using PBE functional and excluding the vdW correction increases the activation energy by 0.09 and 0.06 eV for Au and Pt surfaces, respectively. It is found that the formation of PX on Pt is kinematically more favorable than that of Au(111). Moreover, E_a of Pt is low enough to support the dissociation of PL into PX at low temperatures. These results indicate that the dissociation of PL into PX and H atom, and the recombination of PX and H are reversible processes on Pt surface, while only the latter reaction is reversible on Au(111).

E. Electronic Structure Analysis

The bonding between the molecules and metal surfaces are further investigated by analyzing the charge density and partial density of states (PDOS). The electronic structure analysis of the most stable configurations of PL and PX on Au(111) and Pt(111) will be presented in the following, unless otherwise noted.

1. Charge Density Difference Analysis

The charge density difference or charge displacement due to the adsorption of the molecule on the surface is calculated as

$$\Delta\rho = \rho_{\text{total}} - \rho_{\text{surface}} - \rho_{\text{molecule}} \tag{2}$$

where ρ_{total} is the electronic charge density of PL and PX adsorbed on the surface, ρ_{surface} is the charge density of the Au or Pt slab in the adsorbed configuration without the presence of PL or PX, and ρ_{molecule} is the charge density of the molecule in the adsorbed configuration in vacuum. The atomic positions of the latter two quantities are fixed as they are obtained from the fully optimized systems. For a more quantitative analysis, the average charge density difference, $\Delta\rho_{\text{av}}(z)$, is calculated by averaging over the plane perpendicular to the (111) surface

$$\Delta\rho_{\text{av}}(z) = \int \Delta\rho \; dx \, dy. \tag{3}$$

The charge density differences of the most stable chemisorption and physisorption configurations of PX and PL on Au(111) and Pt(111) surfaces are presented in Fig. 5. When the molecules are adsorbed on these surfaces, there are charge accumulation ($\Delta\rho_{\text{av}}(z) > 0$) and depletion ($\Delta\rho_{\text{av}}(z) < 0$) regions both in the metals and molecules. The physisorption configurations of PL on Au and Pt surfaces, as shown in Fig. 5(a) and (c), respectively, show similar features, where the surface atoms close to O-H bond have larger charge accumulation regions and there are both accumulation (close to surface) and depletion (close to molecule) regions between the surface and molecules. On the other hand, as can be seen in Fig. 5(d) for PX/Au(111), the σ-like adsorption via O atom results in charge depletion regions under the surface and between the molecule and surface. The chemisorption states of PL and PX on Pt(111) exhibit additional bonding between the molecules and surface as shown in Fig. 5(b) and (e). In general, the charge displacement, defined as $\Delta Q = \int |\Delta\rho(z)| \; dz$, is larger for the Pt surface compared to Au surface, and penetrates into the subsurface layer.

The adsorption configurations and energies of BZ and PL on Au(111) surface are similar, thus the charge displacement are close to each other. On the other hand, PX on Au surface has more pronounced charge replacement

due to the O-Au bond formed. Comparing the chemi- to physisorption states of the molecules on Pt(111) surface shows that the charge displacement values for the chemisorbed configurations are significantly larger than those of the physisorption states, which confirms the stronger adsorption energies of the former configurations. The chemisorbed configurations of the molecules on Pt(111) are either n^5-π or n^6-π so the bonding between the C-ring and Pt surface atoms is important, which gives similar charge displacement values for these states. The charge displacement for each configurations is presented in Table S3 and S5 of the supplementary material.[56]

2. Density of States Analysis

The chemistry of adsorption has been analyzed by calculating the DOS of PL and PX on Au and Pt(111) and PDOSs are presented in Figure S7 of the supplementary material.[56] While the adsorption of PL on Au(111) does not significantly change the PDOS of gold atoms on the surface, the chemisorption of PL on Pt(111) has a strong effect on the molecular states of the molecule. Both C and O p-states around the Fermi level are almost bleached and the PDOS between -6 and -4 eV are significantly broaden. The d-states of Pt show small intensity changes around the Fermi level. Similar effects are observed for the chemisorption of PX on Pt(111), with the molecular states decrease in intensity and broaden till -6 eV. The change in the molecular PDOS of PX on Au(111) is quite significant. The physisorption of PL on Pt(111) does not affect the Pt d-states, however C p-states almost bleach together with the O p-states around -2 eV, and the lower energy O p-states decrease the intensity.

IV. CONCLUSIONS

We investigated the adsorption and partial dissociation of phenol on each high symmetry site of Au(111) and Pt(111) by DFT calculations. Two different substrates were chosen to analyze the effect of the metal used. Higher reactivity of Pt results in stronger interactions between the molecules and the substrate compared to those on Au surface.The energy profile of phenol on Pt(111) indicates a stable chemisorption state accompanied by a higher-energy physisorption state, the stability of which depends on the functional used. Chemisorption is mostly due to the interaction between the ring and the surface, while the physisorption is a combination of the vdW interactions not only between the OH and surface, but also between the ring and surface. However, for the most reliable functionals employed (PBE-vdW) the barrier between the two states is extremely low and at low coverage PL molecules are expected to be chemisorbed. Intermolecular interactions at higher coverage may enhance the bistable character of adsorption.

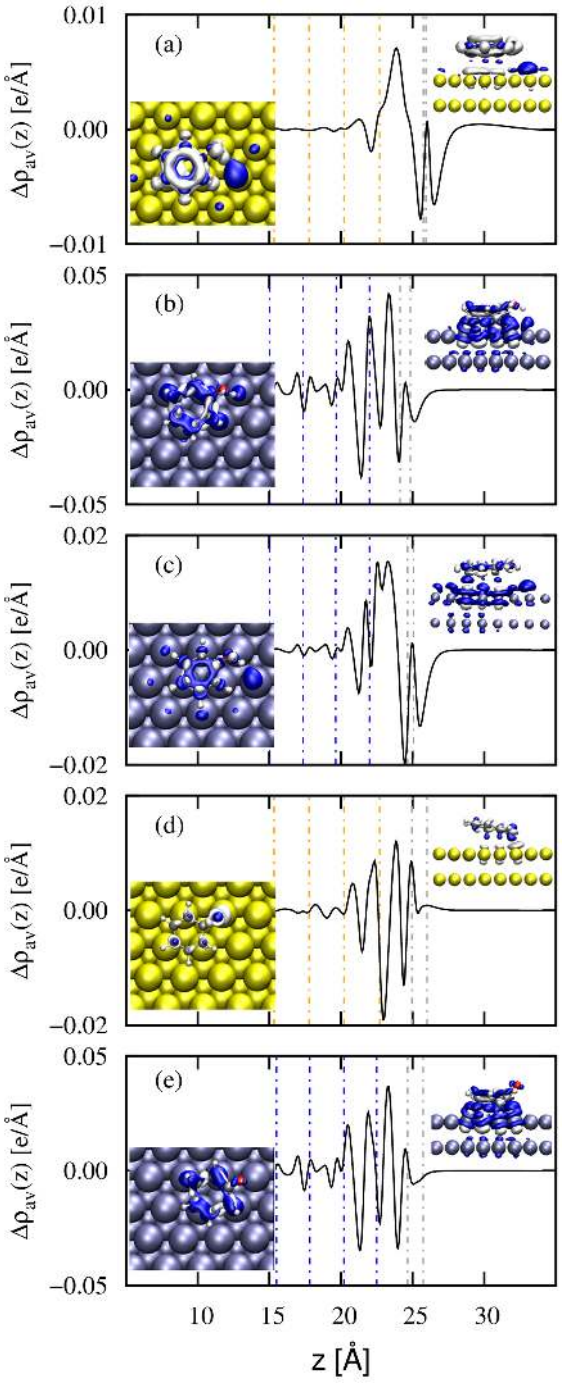

FIG. 5. 1D planar-averaged electronic density difference, $\Delta\rho_{\mathrm{av}}(z)$, for phenol and phenoxy on Au(111) and Pt(111) surfaces with PBE-vdW functional: (a) physisorption of PL on Au(111) with hcp-30 site, (b) chemisorption of PL on Pt(111) with B-30 site, (c) physisorption of PL on Pt(111) with hcp-30 site, (d) physisorption of PX on Au(111) with hcp-30 site, and (e) chemisorption of PX on Pt(111) with B-30 site. The isosurfaces are chosen at 10% of the maximum value. Blue and white regions represent charge accumulation and depletion, respectively. The positions of the surface and subsurface atoms for Au and Pt surface are indicated by orange and blue vertical lines, respectively. The gray vertical lines represent the positions of the tilted molecules.

We also explored the effect of vdW interactions on the energetics of molecules on Au and Pt(111) surfaces using different exchange-correlation functionals: PBE, PBE-vdW, and revPBE-vdW, and PW86-vdW2. In general, PBE and PBE-vdW predict the same adsorption sites and geometries for the strongly adsorbed (chemisorbed) molecules: the most stable configurations are hcp-30 for PL and PX on Au(111) and B-30 site for the chemisorption state of PL and PX on Pt(111) with all functionals used. On the other hand, for the physisorption of PL on Pt(111), these two functionals predict different adsorption sites, i.e., B-30 and hcp-30 sites calculated with PBE and all of the vdW functionals, respectively.

The currently used functionals have similar trends on the adsorption energy of different molecules, i.e., benzene, phenol and phenoxy, on (111) surfaces of Au and Pt. For Au(111), PBE (PBE-vdW) functional always predicts the weakest (strongest) adsorption energy for all molecules, while the adsorption energy of BZ on Au(111) with PW86-vdW2 is within the experimental data. On the other hand, PBE-vdW gives the strongest adsorption energy for all molecules on Au(111), and this functional predicts the adsorption energy of benzene within the experimental range. Remarkably, for benzene, phenol and phenoxy chemisorbed at Pt(111), revPBE-vdW and PW86-vdW2 give weaker adsorption energies than PBE, indicating that these two vdW functionals are too repulsive at short distances and fail to reproduce the correct energy balance between physisorbed and chemisorbed states, which is crucial to describe the interaction between aromatic molecules and transition metals with partially filled d-shell.

The kinetic aspects of the dissociation of phenol into coadsorbed phenoxy and H atom were calculated using the climbing image nudge elastic band. The activation and reaction energies of the dissociation of PL on Au and Pt(111) surfaces are 1.50 and 1.36 eV, and 0.34 and 0.23 eV, respectively.These results indicate that the dissociation of PL is not only kinetically but also thermodynamically unfavorable on Au and Pt(111) surfaces.

ACKNOWLEDGMENTS

We acknowledge the RZG of the Max Planck Society for computational resources. The authors were funded by the MPRG program of the MPG.

[1] S. R. Hartshorn, Ed., *Structural Adhesives: Chemistry and Technology* (Plenum Press, New York, 1986).
[2] G. I. Panov, Cattech **4**, 18 (2000).
[3] N. V. Richardson and P. Hofmann, Vacuum **33**, 793 (1983).
[4] X.-C. Guo and R. J. Madix, Surf. Sci. **341**, 1065 (1995).
[5] J. G. Serafin and C. M. Friend, Surf. Sci. **209**, 163 (1989).
[6] A. C. Liu and C. M. Friend, Surf. Sci. **236**, 349 (1990).
[7] X. Xu and C. M. Friend, J. Phys. Chem. **93**, 8072 (1989).
[8] L. L. Solomon and R. J. Madix, Surf. Sci. **255**, 12 (1991).
[9] J. Lee, S. Ryu, J. S. Ku, and S. K. Kim, J. Chem. Phys. **115**, 10518 (2001).
[10] H. Bu, P. Bertrand, and J. W. Rabalais, J. Chem. Phys. **98**, 5855 (1993).
[11] J. N. Russell, Jr., S. S. Sarvis, and R. E. Morris, Surf. Sci. **338**, 189 (1995).
[12] A. K. Myers and J. B. Benziger, Langmuir **5**, 1270 (1989).
[13] M. Ramsey, G. Rosina, D. Steinmüller, H. H. Graen, and F. P. Netzer, Surf. Sci. **232**, 266 (1990).
[14] K. M. Richard and A. A. Gewirth, J. Phys. Chem. **99**, 12288 (1995).
[15] F. Lu, G. N. Salaita, L. Laguren-Davidson, D. A. Stern, E. Wellner, D. G. Frank, N. Batina, D. C. Zapien, N. Walton, and A. T. Hubbard, Langmuir **4**, 637 (1988).
[16] H. Ihm and J. M. White, J. Phys. Chem. B **104**, 6202 (2000).
[17] M. L. Honkela, J. Björk, and M. Persson, Phys. Chem. Chem. Phys. **14**, 5849 (2012).
[18] G. Li, J. Han, H. Wang, X. Zhu, and Q. Ge, ACS Catal. **5**, 2009 (2015).
[19] L. D. Site, A. Alavi, and C. F. Abrams, Phys. Rev. B **67**, 193406 (2003).
[20] L. M. Ghiringhelli, R. Caputo, and L. D. Site, Phys. Rev. B **75**, 113403 (2007).
[21] H. Orita and N. Itoh, Appl. Catal. A **258**, 17 (2004).
[22] R. O. Lezna, N. R. de Tacconi, S. A. Centeno, and A. J. Arvia, Langmuir **7**, 1241 (1991).
[23] P. Kisliuk, J. Phys. Chem. Solids **3**, 95 (1957).
[24] D. J. Doren and J. C. Tully, Langmuir **4**, 256 (1988).
[25] D. E. Brown, D. J. Moffatt, and R. A. Wolkow, Science **279**, 542 (1998).
[26] F. Mittendorfer, A. Garhofer, J. Redinger, J. Klimes, J. Harl, and G. Kresse, Phys. Rev. B **84**, 201401(R) (2011).
[27] W. Liu, S. N. Filimonov, J. Carrasco, and A. Tkatchenko, Nat. Commun. **4**, 2569 (2013).
[28] R. Peköz, K. Johnston, and D. Donadio, J. Phys. Chem. C **118**, 6235 (2014).
[29] K. Johnston, R. Pekoz, and D. Donadio, Surf. Sci. **644**, 113 (2016).
[30] M. Dion, H. Rydberg, E. Schröder, D. C. Langreth, and B. I. Lundqvist, Phys. Rev. Lett. **92**, 246401 (2004).
[31] A. Gulans, M. J. Puska, and R. M. Nieminen, Phys. Rev.B **79**, 201105(R) (2009).
[32] K. Lee, E. D. Murray, L. Kong, B. I. Lundqvist, and D. C. Langreth, Phys. Rev. B **82**, 081101(R) (2010).
[33] J. P. Perdew, K. Burke, and M. Ernzerhof, Phys. Rev. Lett. **77**, 3865 (1996).
[34] J. Perdew, K. Burke, A. Zupan, and M. Ernzerhof, J. Chem. Phys. **108**, 1522 (1998).
[35] M. Elstner, P. Hobza, T. Frauenheim, S. Suhai, and E. Kaxiras, J. Chem. Phys. **114**, 5149 (2001).
[36] J. Harl and G. Kresse, Phys. Rev. B **77**, 045136 (2008).
[37] A. Tkatchenko and M. Scheffler, Phys. Rev. Lett. **102**, 073005 (2009).
[38] A. T. R. A. DiStasio, Jr., R. Car, and M. Scheffler, Phys. Rev. Lett. **108**, 236402 (2012).
[39] J. P. Perdew and Y. Yang, Phys. Rev. B **33**, 8800(R) (1986).
[40] P. E. Blöchl, Phys. Rev. B **50**, 17953 (1994).
[41] G. Kresse and D. Joubert, Phys. Rev. B **59**, 1758 (1999).
[42] G. Kresse and J. Hafner, Phys. Rev. B **48**, 13115 (1993).
[43] G. Kresse and J. Furthmüller, Comput. Mater. Sci. **6**, 15 (1996).
[44] J. Klimes, D. R. Bowler, and A. Michaelides, Phys. Rev. B **83**, 195131 (2011).
[45] J. Carrasco, W. Liu, A. Michaelides, and A. Tkatchenko, J. Chem. Phys. **140**, 084704 (2014).
[46] E. D. Murray, K. Lee, and D. C. Langreth, J. Chem. Theory Comput. **5**, 2754 (2009).
[47] H. J. Monkhorst and J. D. Pack, Phys. Rev. B **13**, 5188 (1976).
[48] M. Methfessel and A. T. Paxton, Phys. Rev. B **40**, 3616 (1989).
[49] In the AEP curves, the effect of constraining the atomic positions has a small effect on the adsorption energy of molecules on the surfaces. For instance, for PL/Au(111) the minimum of AEP calculated with PBE-vdW is -0.80 eV and the fully optimized value is -0.89 eV. For PL/Pt(111) calculated with PBE-vdW, the chemisorption and physisorption AEP energies are -1.79 and

-1.13 eV, and the fully optimized energies are -1.82 and -1.23 eV, respectively. For PX on Au and Pt(111), the minimum of AEP calculated with PBE-vdW is -1.51 and -2.73 eV, and the adsorption energies of fully relaxed systems are -1.51 and -2.87 eV, respectively.

[50] G. Henkelman and H. Jonsson, J. Chem. Phys. **113**, 9978 (2000).

[51] G. Henkelman and H. Jonsson, J. Chem. Phys. **113**, 9901 (2000).

[52] D. Mei, E. W. Hansen, and M. Neurock, .

[53] A. A. Phatak, W. N. Delgass, F. H. Ribeiro, and W. F. Schneider, J. Phys. Chem. C **113**, 7269 (2009).

[54] D. Donadio, L. M. Ghiringhelli, and L. Delle Site, J. Am. Chem. Soc. **134**, 19217 (2012).

[55] A. Wander, G. Held, R. Q. Hwang, G. S. Blackman, M. L. Xu, P. de Andres, M. A. Van Hove, and G. A. Somorjai, Surf. Sci. **249**, 21 (1991).

[56] See supplementary material at http:xxx for the physi- and chemisorption energies and geometrical details of the systems; relaxed geometries of phenol and phenoxy on Au(111) and Pt(111) using different exchange and correlation functionals; and PDOSs of the most stable configurations.

[57] H. Yildirim, T. Greber, and A. Kara, J. Phys. Chem. C **117**, 20572 (2013).

[58] S. J. Jenkins, Proc. R. Soc. A **465**, 2949 (2009).

[59] As the adsorption energy of benzene and phenol on Au(111) was not particularly dependent on the adsorption site for PBE and PBE-vdW, we decided not to test systematically the molecules for revPBE-vdW and PW86-vdW2.

[60] Even though the energy difference between B-30 and hcp-30 sites calculated by PBE-vdW is very small (0.02 eV), the molecule is distorted from its gas-phase geometry at B-30 site and keeps its planar geometry at hcp-30 site. In contrast, PL on hcp-30 site calculated by PBE is not stable and goes to B-30 site with a chemisorbed geometry. We have also explored the physisorption energies and structural features with the other functionals including vdW interactions. For B-30 site, both PW86-vdW2 and revPBE-vdW functionals yield to chemisorbed structures, while PL on hcp-30 site is stable and keeps its gas phase geometry.

[61] P. Ferrin, S. Kandoi, A. U. Nilekar, and M. Mavrikakis, Surf. Sci. **606**, 679 (2012).

[62] NEB calculations for Au surface with eight reaction intermediates changed the reaction energy by 0.03 eV. Thus, due to the computational cost, we used four reaction intermediates for Pt surface.